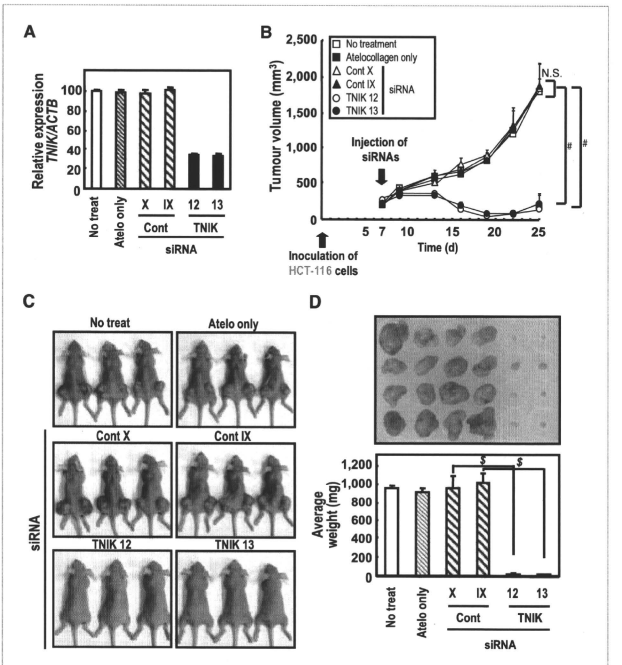

Figure 6. Inhibition of colorectal cancer growth by siRNA against TNIK. A, mRNA expression of *TNIK* in tumors 3 d after the injection with siRNA ($n = 3$ per group). HCT-116 cells were inoculated s.c. into BALB/c nu/nu nude mice. Seven days later, the developed tumors were untreated (No treat) or treated with only atelocollagen (Atelo only), control RNA (X or IX), or siRNA against TNIK (12 or 13). B, the volume of tumors ($n = 8$ per group) was monitored as indicated. #, $P < 0.001$ (Mann-Whitney *U* test); N.S., not significant; bars, SE. C and D, representative appearance of mice (C) and excised tumors (D) 18 d after the injection of siRNA (day 25). Columns in D indicate the average weight of excised tumors ($n = 8$ per group). $, $P < 0.005$ (Mann-Whitney *U* test); bars, SE.

effects of siRNA, we performed rescue experiments. Because the target sequences of both the TNIK siRNAs (12 and 13) are located in the COOH-terminal half of TNIK, we designed plasmid and adenovirus vectors encoding only the NH_2-terminal catalytic domain (amino acids 1–289) of TNIK (i.e., TNIKΔC), which mediates the interaction with TCF4 (Fig. 1B; ref. 21). These constructs successfully rescued the activity of TNIK that had been downregulated by siRNA *in vitro* (Supplementary Fig. S8) and *in vivo* (Supplementary Fig. S12). Knockdown of TNIK did not significantly affect the growth of Wnt-inactive cells [Supplementary Figs. S11 and S6C, β-cateninΔN134(−)], indicating that the suppression of colorectal cancer cell growth is mediated, at least partly, by blockage of Wnt signaling.

We also found that β-catenin overexpression induced TNIK phosphorylation in Wnt-inactive cells (Fig. 3B) and the suppression of β-catenin by siRNA decreased TNIK phosphorylation in colorectal cancer cells (Fig. 3C). These observations indicate that the activation of TNIK is mediated by Wnt signaling. The immunohistochemistry data obtained from clinical samples (Supplementary Fig. S5) support this notion. Activated TNIK is then translocated into the nucleus and augments the transcriptional activity of TCF4. This positive feedback circuit seems to be essential for the continuation of colorectal cancer cell renewal. Elucidation of the molecular pathway that connects the Wnt signal to TNIK, however, will be an issue for future studies.

TNIK was originally identified as a novel member of the germinal center kinase family that interacts with tumor necrosis factor receptor–associated factor-2 (Traf2) and Nck (17). In addition to activation of the c-jun NH_2-terminal kinase pathway, TNIK induces disruption of the filamentous actin structure, thereby inhibiting cell spreading (25). Therefore, the significant suppression of colorectal cancer growth by TNIK siRNA (Fig. 6; Supplementary Figs. S9 and S10) may not be solely attributable to the inhibition of Wnt signaling. In fact, we (Fig. 4A) and others (21) have observed that siRNA targeting TNIK induced only a few-fold decrease of TCF/LEF transcriptional activity in colorectal cancer cells. A full explanation of the molecular mechanisms behind the marked cell growth–suppressive effect will require further detailed studies.

The Wnt signaling pathway is an attractive target for anticancer therapy, but only a few "druggable" targets have

been found in this pathway (43, 44). In the present study, we have clearly shown that TNIK is essential for the continual growth of colorectal cancer. Several synthetic small compounds that bind to the ATP-binding pockets of protein kinases competitively with ATP have been incorporated successfully into oncological practice (18–20). For example, imatinib, which blocks the Bcr-Abl fusion kinase of chronic myeloid leukemia (CML), is currently the first-line therapeutic drug for CML. A new drug targeting TNIK might be effective for the treatment of patients with colorectal cancer.

Disclosure of Potential Conflicts of Interest

No potential conflicts of interest were disclosed.

Acknowledgments

We thank Drs. M. Umikawa and K. Kariya (University of Ryukyus, Okinawa, Japan) for pCIneoHA-TNIK-WT and pCIneoHA-TNIK-K54R, and Dr. T. Ochiya (National Cancer Center Research Institute, Tokyo, Japan) for advice on mouse experiments.

Grant Support

"Program for Promotion of Fundamental Studies in Health Sciences" conducted by the National Institute of Biomedical Innovation of Japan, the "Research on Biological Markers for New Drug Development" conducted by the Ministry of Health, Labor, and Welfare of Japan, and the "Shiseido Female Researcher Science Grant."

The costs of publication of this article were defrayed in part by the payment of page charges. This article must therefore be hereby marked *advertisement* in accordance with 18 U.S.C. Section 1734 solely to indicate this fact.

Received 01/26/2010; revised 04/07/2010; accepted 04/22/2010; published OnlineFirst 06/08/2010.

References

1. Kinzler KW, Vogelstein B. Lessons from hereditary colorectal cancer. Cell 1996;87:159–70.
2. Morin PJ, Sparks AB, Korinek V, et al. Activation of β-catenin-Tcf signaling in colon cancer by mutations in β-catenin or APC. Science 1997;275:1787–90.
3. Sparks AB, Morin PJ, Vogelstein B, Kinzler KW. Mutational analysis of the APC/β-catenin/Tcf pathway in colorectal cancer. Cancer Res 1998;58:1130–4.
4. Peifer M, Polakis P. Wnt signaling in oncogenesis and embryogenesis-a look outside the nucleus. Science 2000;287:1606–9.
5. Polakis P. Wnt signaling and cancer. Genes Dev 2000;14:1837–51.
6. Clevers H. Wnt breakers in colon cancer. Cancer Cell 2004;5:5–6.
7. Behrens J, von Kries JP, Kuhl M, et al. Functional interaction of β-catenin with the transcription factor LEF-1. Nature 1996;382:638–42.
8. Huber O, Korn R, McLaughlin J, Ohsugi M, Herrmann BG, Kemler R. Nuclear localization of β-catenin by interaction with transcription factor LEF-1. Mech Dev 1996;59:3–10.
9. van de Wetering M, Cavallo R, Dooijes D, et al. Armadillo coactivates transcription driven by the product of the Drosophila segment polarity gene dTCF. Cell 1997;88:789–99.
10. Hovanes K, Li TW, Munguia JE, et al. β-Catenin-sensitive isoforms of lymphoid enhancer factor-1 are selectively expressed in colon cancer. Nat Genet 2001;28:53–7.
11. Van der Flier LG, Sabates-Bellver J, Oving I, et al. The intestinal Wnt/TCF signature. Gastroenterology 2007;132:628–32.
12. Korinek V, Barker N, Morin PJ, et al. Constitutive transcriptional activation by a β-catenin-Tcf complex in APC−/− colon carcinoma. Science 1997;275:1784–7.
13. Korinek V, Barker N, Moerer P, et al. Depletion of epithelial stem-cell compartments in the small intestine of mice lacking Tcf-4. Nat Genet 1998;19:379–83.
14. Naishiro Y, Yamada T, Takaoka AS, et al. Restoration of epithelial cell polarity in a colorectal cancer cell line by suppression of β-catenin/T-cell factor 4-mediated gene transactivation. Cancer Res 2001;61:2751–8.
15. Shitashige M, Hirohashi S, Yamada T. Wnt signaling inside the nucleus. Cancer Sci 2008;99:631–7.
16. Shitashige M, Satow R, Honda K, Ono M, Hirohashi S, Yamada T. Regulation of Wnt signaling by the nuclear pore complex. Gastroenterology 2008;134:1961–71, 71 e1–4.
17. Fu CA, Shen M, Huang BC, Lasaga J, Payan DG, Luo Y. TNIK, a novel member of the germinal center kinase family that activates the c-Jun N-terminal kinase pathway and regulates the cytoskeleton. J Biol Chem 1999;274:30729–37.
18. Druker BJ, Guilhot F, O'Brien SG, et al. Five-year follow-up of patients receiving imatinib for chronic myeloid leukemia. N Engl J Med 2006;355:2408–17.
19. Llovet JM, Ricci S, Mazzaferro V, et al. Sorafenib in advanced hepatocellular carcinoma. N Engl J Med 2008;359:378–90.
20. Mok TS, Wu YL, Thongprasert S, et al. Gefitinib or carboplatin-paclitaxel in pulmonary adenocarcinoma. N Engl J Med 2009;361:947–57.
21. Mahmoudi T, Li VS, Ng SS, et al. The kinase TNIK is an essential activator of Wnt target genes. EMBO J 2009;28:3329–40.
22. Idogawa M, Masutani M, Shitashige M, et al. Ku70 and poly (ADP-ribose) polymerase-1 competitively regulate β-catenin and T-cell factor-4-mediated gene transactivation: possible linkage of DNA damage recognition and Wnt signaling. Cancer Res 2007;67:911–8.
23. Shitashige M, Naishiro Y, Idogawa M, et al. Involvement of splicing factor-1 in β-catenin/T-cell factor-4-mediated gene transactivation and pre-mRNA splicing. Gastroenterology 2007;132:1039–54.
24. Sato S, Idogawa M, Honda K, et al. β-Catenin interacts with the FUS proto-oncogene product and regulates pre-mRNA splicing. Gastroenterology 2005;129:1225–36.
25. Taira K, Umikawa M, Takei K, et al. The Traf2- and Nck-interacting kinase as a putative effector of Rap2 to regulate actin cytoskeleton. J Biol Chem 2004;279:49488–96.
26. Huang L, Shitashige M, Satow R, et al. Functional interaction of DNA topoisomerase IIα with the β-catenin and T-cell factor-4 complex. Gastroenterology 2007;133:1569–78.
27. Hatanaka K, Ohnami S, Yoshida K, et al. A simple and efficient method for constructing an adenoviral cDNA expression library. Mol Ther 2003;8:158–66.
28. Idogawa M, Yamada T, Honda K, Sato S, Imai K, Hirohashi S. Poly(ADP-ribose) polymerase-1 is a component of the oncogenic T-cell factor-4/β-catenin complex. Gastroenterology 2005;128:1919–36.
29. Aoki K, Barker C, Danthinne X, Imperiale MJ, Nabel GJ. Efficient generation of recombinant adenoviral vectors by Cre-lox recombination *in vitro*. Mol Med 1999;5:224–31.
30. Zhang WW, Koch PE, Roth JA. Detection of wild-type contamination in a recombinant adenoviral preparation by PCR. Biotechniques 1995;18:444–7.
31. Takeshita F, Minakuchi Y, Nagahara S, et al. Efficient delivery of small interfering RNA to bone-metastatic tumors by using atelocollagen *in vivo*. Proc Natl Acad Sci U S A 2005;102:12177–82.
32. Minakuchi Y, Takeshita F, Kosaka N, et al. Atelocollagen-mediated synthetic small interfering RNA delivery for effective gene silencing *in vitro* and *in vivo*. Nucleic Acids Res 2004;32:e109.

33. Bergers G, Javaherian K, Lo KM, Folkman J, Hanahan D. Effects of angiogenesis inhibitors on multistage carcinogenesis in mice. Science 1999;284:808–12.
34. Wissing J, Jansch L, Nimtz M, et al. Proteomics analysis of protein kinases by target class-selective prefractionation and tandem mass spectrometry. Mol Cell Proteomics 2007;6:537–47.
35. Naishiro Y, Yamada T, Idogawa M, et al. Morphological and transcriptional responses of untransformed intestinal epithelial cells to an oncogenic β-catenin protein. Oncogene 2005;24:3141–53.
36. Yan D, Wiesmann M, Rohan M, et al. Elevated expression of axin2 and hnkd mRNA provides evidence that Wnt/β-catenin signaling is activated in human colon tumors. Proc Natl Acad Sci U S A 2001; 98:14973–8.
37. He TC, Sparks AB, Rago C, et al. Identification of c-MYC as a target of the APC pathway. Science 1998;281:1509–12.
38. Mann B, Gelos M, Siedow A, et al. Target genes of β-catenin-T cell-factor/lymphoid-enhancer-factor signaling in human colorectal carcinomas. Proc Natl Acad Sci U S A 1999;96:1603–8.
39. Crawford HC, Fingleton BM, Rudolph-Owen LA, et al. The metalloproteinase matrilysin is a target of β-catenin transactivation in intestinal tumors. Oncogene 1999;18:2883–91.
40. Tetsu O, McCormick F. β-Catenin regulates expression of cyclin D1 in colon carcinoma cells. Nature 1999;398:422–6.
41. Haegebarth A, Clevers H. Wnt signaling, lgr5, and stem cells in the intestine and skin. Am J Pathol 2009;174:715–21.
42. Radtke F, Clevers H. Self-renewal and cancer of the gut: two sides of a coin. Science 2005;307:1904–9.
43. Emami KH, Nguyen C, Ma H, et al. A small molecule inhibitor of β-catenin/CREB-binding protein transcription [corrected]. Proc Natl Acad Sci U S A 2004;101:12682–7.
44. Huang SM, Mishina YM, Liu S, et al. Tankyrase inhibition stabilizes axin and antagonizes Wnt signalling. Nature 2009;461:614–20.

Cancer Epidemiology, Biomarkers & Prevention

Reduced Plasma Level of CXC Chemokine Ligand 7 in Patients with Pancreatic Cancer

Junichi Matsubara[1,2], Kazufumi Honda[1], Masaya Ono[1], Yoshinori Tanaka[3], Michimoto Kobayashi[3], Giman Jung[3], Koji Yanagisawa[4], Tomohiro Sakuma[4], Shoji Nakamori[5], Naohiro Sata[6], Hideo Nagai[6], Tatsuya Ioka[7], Takuji Okusaka[8], Tomoo Kosuge[8], Akihiko Tsuchida[9], Masashi Shimahara[10], Yohichi Yasunami[11], Tsutomu Chiba[2], Setsuo Hirohashi[1], and Tesshi Yamada[1]

Abstract

Background: Early detection is essential to improve the outcome of patients with pancreatic cancer. A noninvasive and cost-effective diagnostic test using plasma/serum biomarkers would facilitate the detection of pancreatic cancer at the early stage.

Methods: Using a novel combination of hollow fiber membrane–based low-molecular-weight protein enrichment and LC-MS-based quantitative shotgun proteomics, we compared the plasma proteome between 24 patients with pancreatic cancer and 21 healthy controls (training cohort). An identified biomarker candidate was then subjected to a large blinded independent validation ($n = 237$, validation cohort) using a high-density reverse-phase protein microarray.

Results: Among a total of 53,009 MS peaks, we identified a peptide derived from CXC chemokine ligand 7 (CXCL7) that was significantly reduced in pancreatic cancer patients, showing an area under curve (AUC) value of 0.84 and a P value of 0.00005 (Mann–Whitney U test). Reduction of the CXCL7 protein was consistently observed in pancreatic cancer patients including those with stage I and II disease in the validation cohort ($P < 0.0001$). The plasma level of CXCL7 was independent from that of CA19-9 (Pearson's $r = 0.289$), and combination with CXCL7 significantly improved the AUC value of CA19-9 to 0.961 ($P = 0.002$).

Conclusions: We identified a significant decrease of the plasma CXCL7 level in patients with pancreatic cancer, and combination of CA19-9 with CXCL7 improved the discriminatory power of the former for pancreatic cancer.

Impact: The present findings may provide a new diagnostic option for pancreatic cancer and facilitate early detection of the disease. *Cancer Epidemiol Biomarkers Prev; 20(1); 1–12. ©2011 AACR.*

Authors Affiliations: [1]Chemotherapy Division, National Cancer Center Research Institute, Tokyo, [2]Department of Gastroenterology and Hepatology, Kyoto University Graduate School of Medicine, Kyoto, [3]New Frontiers Research Laboratories, Toray Industries, Kamakura, [4]BioBusiness Group, Mitsui Knowledge Industry, Tokyo, [5]Department of Surgery, Osaka National Hospital, National Hospital Organization, Osaka, [6]Department of Surgery, Jichi Medical University, Shimotsuke, [7]Department of Hepatobiliary and Pancreatic Oncology, Osaka Medical Center for Cancer and Cardiovascular Diseases, Osaka, [8]Hepatobiliary and Pancreatic Oncology and Hepatobiliary and Pancreatic Surgery Divisions, National Cancer Center Hospital, Tokyo, [9]Third Department of Surgery, Tokyo Medical University, Tokyo, [10]Department of Oral Surgery, Osaka Medical College, Osaka, and [11]Department of Regenerative Medicine and Transplantation, Fukuoka University Faculty of Medicine, Fukuoka, Japan

Note: Supplementary data for this article are available at Cancer Epidemiology, Biomarkers & Prevention Online (http://cebp.aacrjournals.org/).

Corresponding Author: Tesshi Yamada, Chemotherapy Division, National Cancer Center Research Institute, 5-1-1 Tsukiji, Chuo-ku, Tokyo 104-0045, Japan. Phone: 81-3-3542-2511; Fax: 81-3-3547-6045. E-mail: tyamada@ncc.go.jp

doi: 10.1158/1055-9965.EPI-10-0397

Introduction

Pancreatic adenocarcinoma is one of the most aggressive and lethal of diseases. The overall 5-year survival rate of patients with pancreatic cancer is less than 5%, which is the lowest among the more common cancers (1, 2), and the disease is the fifth leading cause of cancer death in Japan and the fourth in the United States, with greater than 23,000 estimated annual deaths in Japan and greater than 33,000 in the United States (3, 4). The 5-year survival rate of patients who were able to undergo surgical resection reaches 20% to 40% (5, 6), but the majority of pancreatic cancer patients have already developed lymph node and/or distant organ metastasis at their first clinical presentation, and only about 20% of patients are able to undergo radical resection (7, 8). The introduction of gemcitabine has significantly improved the overall survival of patients with unresectable pan-

creatic cancer, but their median survival period still remains about 6 months (9–11). These statistics demonstrate that early detection is essential for improving the outcome of patients with pancreatic cancer.

Computed tomography (CT), magnetic resonance imaging (MRI), and positron emission tomography (PET) are not cost-effective for the screening of pancreatic cancer because of the relatively low incidence of the disease. If a noninvasive and cost-effective screening test employing plasma/serum markers could be devised, it would significantly facilitate the early detection of pancreatic cancer. However, no biomarker suitable for screening of pancreatic cancer is currently available (12). CA19-9 is an established biomarker useful for the follow-up of pancreatic cancer patients receiving treatment, but has not been recommended for cancer screening because of its insufficient sensitivity and specificity (7, 13). Therefore, the discovery of a new biomarker that would be able to supplement CA19-9 has been anticipated.

Recently, advanced proteomic technologies based on mass spectrometry (MS) have been increasingly applied to studies of clinical samples to identify new biomarkers of various diseases (14) including pancreatic cancer (12, 15). It is anticipated that alterations in the protein content of clinical samples reflect the biological status of patients more directly than those in mRNA (16). We previously developed a new shotgun proteome platform, 2-Dimensional Image Converted Analysis of Liquid chromatography and mass spectrometry (2DICAL; ref. 17). 2DICAL is highly advantageous for clinical proteomics because of its high quantification accuracy and throughput. Using 2DICAL, we have been able to identify several plasma/serum biomarkers useful for cancer detection and therapy tailoring (18–20).

The serum/plasma proteome accumulates a large variety of disease-related alterations and is considered to be a rich source of biomarkers. However, for proteomic analysis of blood samples, the efficient depletion of a handful of particularly abundant proteins, such as albumin and immunoglobulin, has been challenging (21). Recently, we developed a novel method for the pretreatment of serum/plasma using the high-performance hollow fiber membrane (HFM) filtration technique (22). This method employs multistage filtration and cascaded cross-flow processes, enabling fully automated separation of proteins below a predetermined molecular weight (22). As the more abundant plasma proteins generally have relatively large molecular weights, they can be efficiently eliminated using the HFM technique.

To identify new biomarkers that might be useful for the early detection of patients with pancreatic cancer, we performed a comprehensive analysis of low-molecular-weight (LMW) plasma proteins in these patients using a combination of the HFM and 2DICAL techniques. A large variety of LMW proteins are known to be secreted from diseased tissues and can serve as good diagnostic biomarkers for various diseases (23, 24). Here, we report the identification and validation of an LMW chemotactic cytokine, CXC chemokine ligand 7 (CXCL7), as a novel biomarker for pancreatic cancer.

Patients and Methods

Plasma samples

Plasma samples were collected prospectively from 282 individuals (K. Honda, T. Okusaka, K. Felix, S. Nakamori, N. Sata, H. Nagai, et al., manuscript submitted) including healthy volunteers and newcomers to mainly departments of gastroenterology between August 2006 and October 2008 at the following 7 hospitals in Japan: National Cancer Center Hospital (NCCH), Osaka National Hospital (ONH), Jichi Medical School Hospital, Osaka Medical College (OMC), Tokyo Medical University Hospital (TMUH), Osaka Medical Center for Cancer and Cardiovascular Diseases, and Fukuoka University Hospital. This multi-institutional collaborative study group was organized by the "Third-Term Comprehensive Control Research for Cancer" conducted by the Ministry of Health, Labour and Welfare of Japan, and as part of the International Cancer Biomarker Consortium (25). The procedures used for collection and storage were kept uniform for all plasma samples.

The 282 plasma samples were split into 2 study sets (referred to as the training and validation cohorts). The training cohort comprised 45 individuals including patients with untreated pancreatic cancer at NCCH ($n = 19$) and TMUH ($n = 5$), and healthy controls at NCCH ($n = 2$), TMUH ($n = 9$), OMC ($n = 6$), and ONH ($n = 4$). The validation cohort comprised 237 individuals including 140 patients with pancreatic cancer, 10 patients with chronic pancreatitis, and 87 healthy controls. All patients diagnosed as having pancreatic cancer had histologically or cytologically proven ductal adenocarcinoma. Demographic and laboratory data are summarized in Table 1. The staging of pancreatic cancer was in accordance with the TNM classification of the International Union against Cancer (UICC).

Blood was collected in a tube with EDTA at the time of diagnosis. The plasma was separated by centrifugation and frozen at −80°C until analysis. Samples showing macroscopic evidence of hemolysis were excluded from the current analysis. Written informed consent was obtained from every subject before blood collection. The protocol of this study was reviewed and approved by the institutional ethics committee boards of each participating institution.

Depletion of high-molecular-weight plasma proteins

The plasma samples of the training cohort were filtered through a 0.22-μm pore size filter. Five hundred microliters of the sample was diluted by adding 3.5 mL of 25 mmol/L of ammonium bicarbonate buffer (pH 8.0). The total 4 mL of the diluted plasma was processed as previously described (22). After 1 hour of fully automated operation, LMW proteins with molecular weights smaller than 60 kDa were recovered (Supplementary Fig. S1) and lyophilized.

Table 1. Clinicopathologic characteristics of individuals in training and validation cohorts

	Training cohort (n = 45)			Validation cohort (n = 237)				
	Healthy control	Cancer	P	Healthy control	Cancer	P^f	Chronic pancreatitis	P^f
No. of patients	21	24		87	140		10	
Sex, n			0.205[a]			0.485[a]		0.487[a]
Male	17	15		56	83		8	
Female	4	9		31	57		2	
Age, y			<0.001			<0.001		0
mean (SD)	40 (13)	64 (7)		43 (16)	66 (10)		58 (13)	
Tumor location			NA			NA		NA
Head	–	14		–	59		–	
Body or tail	–	10		–	76		–	
Unknown	–	0		–	5		–	
Clinical stage			NA			NA		NA
I	–	1		–	5		–	
II	–	6		–	25		–	
III	–	4		–	40		–	
IV	–	13		–	70		–	
CA19-9 median, U/mL	5.5	1,109	<0.001	10.2	476	<0.001	5.2	0.06
>37.0 (ULN), no. of patients	2	19		4	110		0	
DUPAN-2 median, U/mL	12	540	<0.001	12	375	<0.001	25	<0.001
>150.0 (ULN), no. of patients	1	19		0	92		1	
CEA median, ng/mL	1.7	6.0	<0.001	1.7	3.5	<0.001	2.6	0.110
>5.0 (ULN), no. of patients	1	12		5	49		1	
Total bilirubin median, mg/dL	0.5	0.4	0.688	0.5	0.5	0.574	0.5	0.4
>1.2 (ULN), no. of patients	0	2		4	18		0	
CXCL7								
Mass spectrometry peak intensity[b], mean (SD)	332 (240)	138 (346)	<0.001[d]	–	–			
Protein intensity[c], mean (SD)	4.14 (0.18)	3.83 (0.28)	<0.001[e]	4.18 (0.14)	3.92 (0.28)	<0.001[e]	3.99 (0.10)	<0.001[e]

NOTE. Wilcoxon test was applied to assess differences in values.

Abbreviations: CEA, carcinoembryonic antigen; NA, not applicable; ULN, upper limit of normal.

[a]Calculated by Fisher's exact test.

[b]Intensity of the corresponding peak measured by quantitative mass spectrometry.

[c]Measured using reverse-phase protein microarrays (logarithmic variable).

[d]Calculated by Mann-Whitney U-test.

[e]Calculated by Welch's t test.

[f]Compared with healthy controls.

The concentration of β2-microglobulin before and after HFM treatment was measured using an ELISA kit (Human Beta-2 Microglobulin ELISA Kit: Alpha Diagnostic Intl. Inc.) to ensure consistent recovery.

Liquid chromatography/mass spectrometry

The HFM-treated samples were digested with sequencing grade-modified trypsin (Promega) and analyzed in duplicate using a nano-flow high-performance liquid chromatography (HPLC; NanoFrontier nLC, Hitachi High-technologies) connected to an electrospray ionization quadrupole time-of-flight (ESI-Q-TOF) mass spectrometer (Q-Tof Ultima, Waters).

MS peaks were detected, normalized, and quantified using the in-house 2DICAL software package, as described previously (17). A serial identification (ID) number was applied to each of the MS peaks detected (1 to 53,009). The stability of LC-MS was monitored by calculating the correlation coefficient (CC) and coefficient of variance (CV) of every measurement. The mean CC ± SD and CV ± SD for all 53,009 peaks observed in the 45 duplicate runs were as high as 0.946 ± 0.042 and as low as 0.053 ± 0.010, respectively.

Protein identification by tandem MS (MS/MS)

Peak lists were generated using the Mass Navigator software package (version 1.2; Mitsui Knowledge Industry) and searched against the SwissProt database (downloaded on April 22, 2009) using the Mascot software package (version 2.2.1; Matrix Science). The search parameters used were as follows. A database of human proteins was selected. Trypsin was designated as the enzyme, and up to 1 missed cleavage was allowed. Mass tolerances for precursor and fragment ions were ± 0.6 Da and ± 0.2 Da, respectively. The score threshold was set to $P < 0.05$ based on the size of the database used in the search. If a peptide was matched to multiple proteins, the protein name with the highest Mascot score was selected.

Western blot analysis

Primary antibodies used were a rabbit polyclonal antibody against platelet basic protein (PBP) precursor (Sigma) and a mouse monoclonal antibody against human complement C3b-α (PROGEN). The anti-PBP antibody recognizes all the known cleaved forms of PBP including CTAP-III and NAP-2. Six microliters of 1:10 diluted plasma sample was separated by SDS-PAGE and electroblotted onto a polyvinylidene difluoride (PVDF) membrane. The membrane was then incubated with the primary antibody and subsequently with the relevant horseradish peroxidase (HRP)-conjugated anti-rabbit or anti-mouse IgG, as described previously (26, 27). Blots were developed using an enhanced chemiluminescence (ECL) detection system (GE Healthcare).

Reverse-phase protein microarray

The plasma samples were passed through IgY microbeads (Seppro-IgY12, Sigma-Aldrich) using an automated Magtration System SA-1 (Precision System Science) in accordance with the manufacturer's instructions to reduce the 12 most abundant plasma proteins. The flow-through portion was serially diluted 1:50, 1:100, 1:200, and 1:400 using a Biomek 2000 Laboratory Automation Robot (Beckman Coulter) and randomly plotted onto ProteoChip glass slides (Proteogen) in quadruplicate in a 6,144-spot/slide format using a Protein Microarrayer Robot (Kaken Geneqs). The spotted slides were incubated overnight with the anti-PBP precursor antibody and then with biotinylated anti-rabbit IgG (Vector Laboratories) and subsequently with streptavidin-HRP conjugate (GE Healthcare). The peroxidase activity was detected using the Tyramide Signal Amplification (TSA) Cyanine 5 System (PerkinElmer). The slides were counterstained with Alexa Fluor 546-labeled goat anti-human IgG (Invitrogen; spotting control).

The stained slides were scanned on a microarray scanner (InnoScan 700AL; Innopsys). Fluorescence intensity, determined as the mean value of quadruplicate samples, was determined using the Mapix software package (Innopsys). All determined intensity values were transformed into logarithmic variables.

The reproducibility of the reverse-phase protein microarray assay was determined by repeating the same experiment, as reported previously (28). A plasma sample after reduction of the 12 most abundant plasma proteins was serially diluted within a range of 25- to 6,400-fold. Each diluted sample was spotted in quadruplicate onto glass slides and blotted with the anti-PBP antibody. In a representative quality control experiment, the CC value was 0.980 between days and the median CV was 0.047 among the quadruplicates.

Multiplex assay

The levels of CXCL7 in plasma samples were measured using a Milliplex Human Cytokine/Chemokine panel III kit (Millipore) in accordance with the manufacturer's instructions.

Statistical analysis

Statistical significance of intergroup differences was assessed with the Wilcoxon test, Mann–Whitney U test, Welch's t test, or Fisher's exact test, as appropriate. The area under the curve (AUC) of the receiver-operating characteristic (ROC) was calculated for each marker to evaluate its diagnostic significance. A composite index of 2 markers was generated using the results of multivariate logistic regression analysis, which also enabled the calculation of sensitivity, specificity, and the ROC curve. Statistical analyses were performed using an open-source statistical language R (version 2.7.0) with the optional module Design package.

Results

Plasma proteins associated with pancreatic cancer

A plasma sample from 1 healthy volunteer was processed 3 times using the HFM filtration technique. The concentration of β2-microglobulin before and after HFM

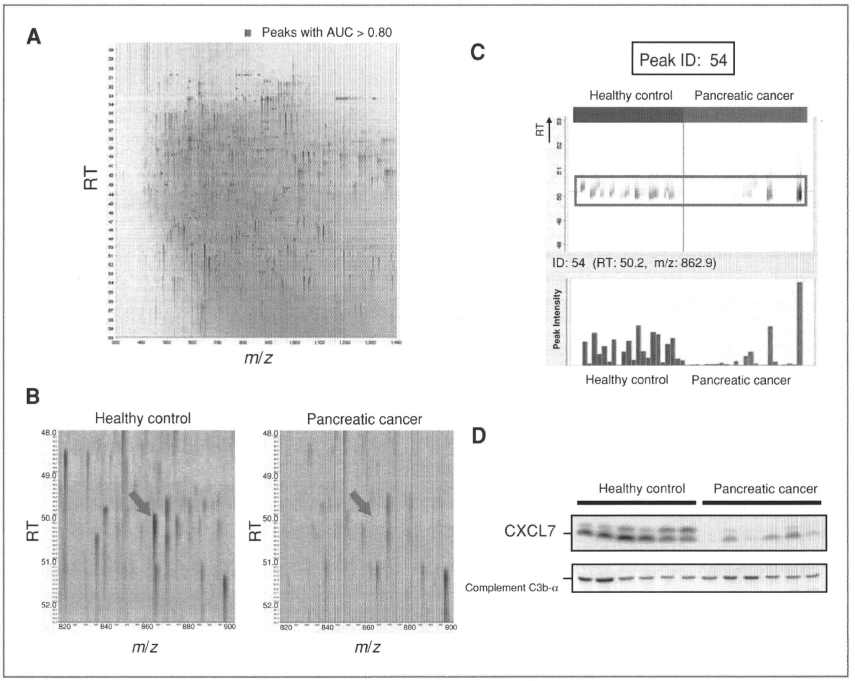

Figure 1. A, 2-dimensional display of all (>53,000) the MS peaks with m/z values along the x-axis and RT of LC along the y-axis. The peaks are displayed with a bin size of 1.0 m/z. The 140 MS peaks whose mean intensity of duplicates that distinguished pancreatic cancer patients from healthy controls with AUC values of greater than 0.800 are highlighted in red. B, CXCL7-derived MS peak (ID 54, at 863 m/z and 50.2 minutes) in representative patients from the cancer and control groups. C, CXCL7-derived MS peak (ID 54) in 45 duplicate LC-MS runs [patients with pancreatic cancer (red) and healthy controls (blue)] aligned along the RT of LC. Columns represent the mean intensity of duplicates (bottom). D, detection of CXCL7 and complement C3b-α (loading control) by Western blotting. Multiple bands for CXCL7 indicate the presence of proteolytic products.

treatment was measured. The recovery rates were 25.11%, 25.73%, and 29.16%, respectively. Although the rates were seemingly low, the HFM treatment was highly reproducible with a CV of 0.081 and the amount of β2-microglobulin relative to total protein was increased 150 to 200-fold after HFM treatment.

To identify a diagnostic biomarker for pancreatic cancer, we compared the plasma LMW proteome between 24 patients with pancreatic cancer and 21 healthy controls (training cohort) using 2DICAL. Among a total of 53,009 independent MS peaks detected within the range 250 to 1,600 m/z and within a time range of 20 to 70 minutes, we found that 140 peaks had discriminatory ability with a AUC of above 0.800. Figure 1A is a representative 2-dimensional view of all the MS peaks displayed with m/z along the x-axis and the retention time (RT) of LC along the y-axis.

Twenty-five MS/MS spectra acquired from those 140 peaks were recurrently matched to 10 proteins in the database with a Mascot score of greater than 30 (Supplementary Table S1). Notably, one MS peak (ID 54) matched the amino acid sequence of the *CXCL7* gene product (Swiss-Prot_P02775) with the highest score of 99.6 (Supplementary Fig. S2). Figure 1B shows the CXCL7-derived MS peak (ID 54, at 863 m/z and 50.2 minutes) that appeared in a representative pancreatic cancer patient and a healthy individual. Figure 1C demonstrates the distribution of the MS peak (ID 54) in patients with pancreatic cancer (red) and healthy controls (blue) in the training cohort (AUC = 0.839; $P = 4.54 \times 10^{-5}$; Mann–Whitney U test). The differential expression and identification of CXCL7 was confirmed by immunoblotting (Fig. 1D).

Validation of reduced CXCL7 in pancreatic cancer patients

The level of plasma CXCL7 was quantified in 12 patients with pancreatic cancer and 12 healthy individuals in the training cohort using multiplex assay. Consistent with 2DICAL, CXCL7 was found to be significantly decreased in patients with pancreatic cancer (mean ± SD, 744 ± 182 ng/mL) in comparison with healthy controls (1,355 ± 386 ng/mL; $P = 0.0003$). To further verify and validate the reduction of plasma CXCL7 in pancreatic cancer patients, 280 plasma samples [including 43 samples from the training cohort and new 237 samples (validation cohort)] were randomly plotted into a reverse-phase protein microarray and blotted with anti-PBP antibody (Fig. 2). Two samples from healthy controls in the training cohort were excluded due to an insufficient sample volume. Quadruplicate spots for representative cases and controls with high and low levels of CXCL7 are shown in the right panels of Figure 2.

The results of reverse-phase protein microarray were well correlated with those of multiplex assay (Pearson's $r = 0.65$; $P = 0.0006$; Supplementary Fig. S3). Microarray analysis also showed a significant reduction of the plasma CXCL7 level in the pancreatic cancer patients of the training cohort ($P = 5.96 \times 10^{-5}$; Welch's t test; Fig. 3A and Table 1) with an AUC value of 0.872 (95% CI: 0.732–0.951; Fig. 3B). The reduction of plasma CXCL7 was further validated in a larger independent cohort (validation cohort; $P = 1.40 \times 10^{-16}$; Fig. 3C and AUC value of 0.850, 95% CI: 0.792–0.895; Fig. 3B). Because there was a difference in age distribution between the cancer patients and healthy controls of the validation cohort (Table 1), we performed a subgroup analysis of 79 pancreatic cancer patients (median age, 61) and 20 healthy controls (median age, 60) aged 50 to 70 years. The reduction of plasma CXCL7 in patients with pancreatic cancer was statistically significant even in this subgroup ($P = 0.0001$), indicating that the decrease of the CXCL7 level was not merely due to the difference of age distribution between the pancreatic cancer patients and controls.

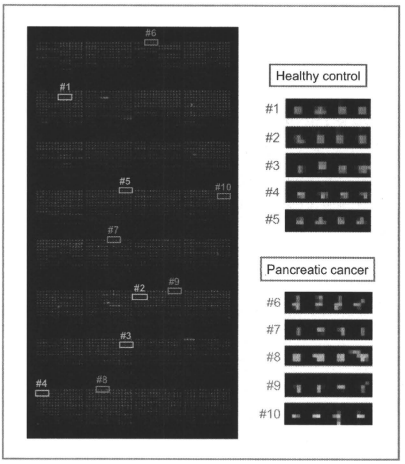

Figure 2. Image of a representative reverse-phase protein microarray slide stained with anti-PBP antibody (left). Samples were randomly assigned, and quadruplicate spots from representative patients with high and low levels of CXCL7 were extracted (right).

CXCL7 was significantly reduced in patients with any stage of pancreatic cancer (Table 2), including those with stage I (<0.001) and II (<0.001) disease. The significant alteration evident in early-stage patients indicated that the reduction of plasma CXCL7 is an early event in pancreatic carcinogenesis and may precede the development of cancer. The persistent presence of inflammation is known to promote carcinogenesis in various organs,

Table 2. Plasma CXCL7 level according to clinical stage of pancreatic cancer

	Pancreatic cancer patients				Healthy controls
	Stage I	Stage II	Stage III	Stage IV	
Training cohort					
No. of cases	1	6	4	13	19[b]
CXCL7[a], mean (SD)	3.67 (-)	3.93 (0.24)	3.75 (0.17)	3.82 (0.33)	4.14 (0.18)
P (vs. healthy controls)	0.01	0.01	<0.001	<0.001	
Validation cohort					
No. of cases	5	25	40	70	87
CXCL7[a], mean (SD)	3.89 (0.34)	3.96 (0.25)	4.02 (0.18)	3.86 (0.32)	4.18 (0.14)
P (vs. healthy controls)	<0.001	<0.001	<0.001	<0.001	

NOTE. Welch's t test was applied to assess differences in values.
[a]Measured using reverse-phase protein microarrays.
[b]Two patients whose samples were not available for reverse-phase protein microarrays were excluded.

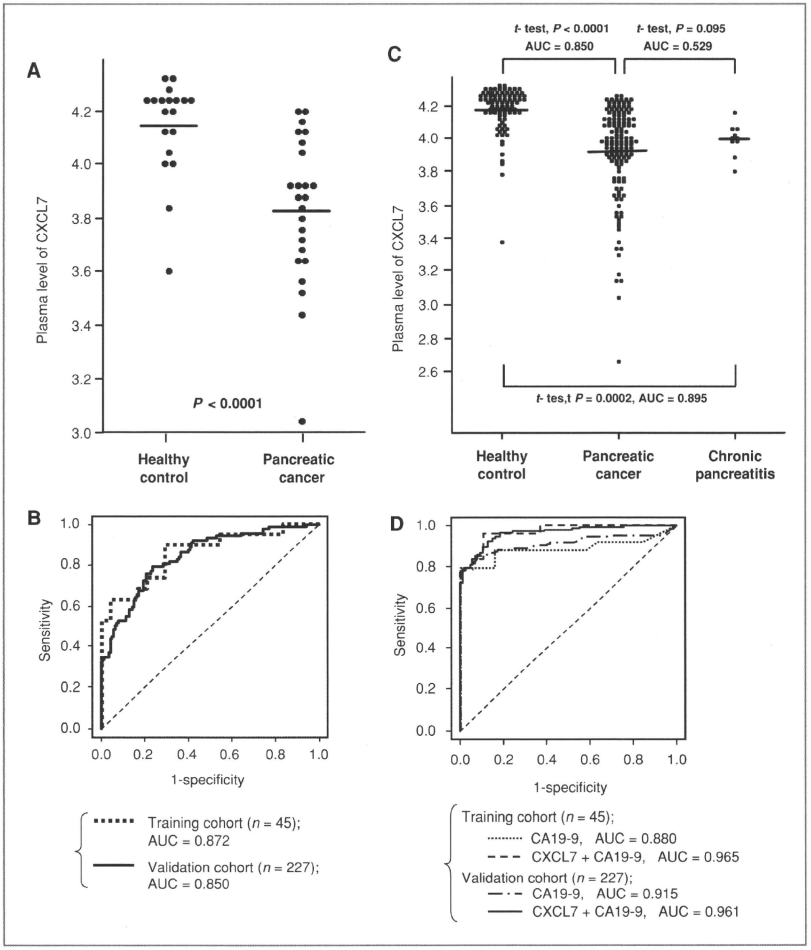

Figure 3. A and C, plasma levels (in arbitrary units) of CXCL7 in healthy controls, patients with pancreatic cancer, and patients with chronic pancreatitis in the training (A) and validation (C) cohorts. Horizontal lines represent the average levels of CXCL7. B, ROC analyses for the discriminatory value of CXCL7 in the training (dotted line) and validation (solid line) cohorts. D, ROC analyses for the discriminatory value of CA19-9 and the composite index of CA19-9 and CXCL7 in the training and validation cohorts.

and chronic pancreatitis is suspected to be one a precancerous condition for pancreatic cancer, although opinions on this issue vary. We measured the plasma level of CXCL7 in a small number of patients diagnosed as having chronic pancreatitis ($n = 10$) using the reverse-phase protein microarray (Table 1). The CXCL7 levels in patients with chronic pancreatitis were significantly lower than those in healthy controls ($P = 0.0002$), but slightly higher than those in patients with pancreatic cancer ($P = 0.095$; Fig. 3C).

Complementation of CA19-9 by CXCL7

CA19-9 is an established biomarker that has long been used for the diagnosis of pancreatic cancer. We found that the levels of CXCL7 and CA19-9 were not mutually correlated (Pearson's $r = 0.289$) and that combination with CXCL7 significantly improved the ability of CA19-9 to distinguish patients with pancreatic cancer from healthy controls: the AUC value improved to 0.965 (95% CI: 0.865–0.994) in the training cohort ($P = 0.026$) and to 0.961 (0.932–0.979) in the validation cohort ($P = 0.002$; Fig. 3D). The AUC values of CA19-9 in the 2 cohorts (Fig. 3D) were comparable with those reported previously (29–31).

Even among individuals with normal levels of CA19-9 (<37 U/mL; a cutoff value widely used in clinical practice), CXCL7 was significantly reduced in pancreatic cancer patients in both the training [$P = 0.014$ and AUC = 0.853 (95% CI: 0.650–0.957; Fig. 4A and B)] and validation [$P < 0.0001$ and AUC = 0.834 (95% CI: 0.747–0.899; Fig. 4B and C)] cohorts.

Because of the low prevalence of pancreatic cancer, any screening biomarker must have high specificity (32). The sensitivity/specificity of CA19-9 (cutoff: 37 U/mL) were 79%/89% in the training cohort and 79%/95% in the validation cohort, consistent with previous reports (32). If we defined the cutoff for CXCL7 as a level at which 95% of healthy individuals would be excluded, 83% of pancreatic cancer patients in the training cohort and 84% in the validation cohort would be detected using the combination of CXCL7 and CA19-9 (Supplementary Table S2).

Discussion

Early detection and subsequent radical surgical resection would most likely provide a chance of cure for patients with pancreatic cancer (7). However, patients with early-stage pancreatic cancer are generally asymptomatic and have little opportunity to undergo imaging and/or other diagnostic procedures until their disease becomes advanced. If a sensitive, but minimally invasive and cost-effective, plasma/serum test were available, it would be effective for alerting patients with early pancreatic cancer and offer them a chance to receive prompt and effective medical attention. In the present study, we compared the plasma LMW proteome between patients with pancreatic cancer and healthy controls using a new proteome platform, 2DICAL (Fig. 1), and found a significant decrease of the plasma CXCL7 level in patients with pancreatic cancer (Fig. 1B and C). The result of quantitative LC-MS was then verified using 3 different methods: immunoblotting (Fig. 1D), multiplex, and reverse-phase protein microarray (Figs. 2 and 3) assays. We further validated the significant decrease of CXCL7 in a larger independent cohort (validation cohort). The level of plasma CXCL7 was confirmed to be decreased reproducibly in patients with pancreatic cancer including those with Stage I and II disease (Table 2). CXCL7 did not surpass the sensitivity of CA19-9, but was able to supplement it. Combination with CXCL7 significantly improved the sensitivity of CA19-9 (Fig. 3D and Supplementary Table S2).

In addition to 2DICAL, we utilized 2 state-of-the-art proteome technologies. The proteome analysis of plasma/serum samples has been hampered by the prominence of a handful of abundant proteins such as albumin and immunoglobulin. It is anticipated that the remaining proteins contain an unexplored archive of disease-driven information, but account for only about 1% of the entire human plasma proteome (24). To reduce the complexity of the plasma proteome, we used HFM filtration technology. Our HFM devise can separate and concentrate LMW plasma proteins in a fully automated manner (22) and allows identification of any biomarker candidate that is present at a level of 1 μg/mL. This discovery justifies the future application of the HFM system to more detailed proteome studies aimed at plasma/serum biomarker discovery. The other technology we employed is high-density reverse-phase protein microarray. The protein content of any human sample varies according to the individual, and therefore it is essential to distinguish biomarker candidates from simple interindividual heterogeneity. However, such distinction is possible only by comparing a statistically sufficient number of cases and controls. Our high-density protein microarrays require a minimal sample volume of the nanoliter order and make it possible to measure the quantity of any candidate biomarker protein in a statistically sufficient number of cases and controls (>300 samples; ref. 28) for judgment of its clinical potential in a single experiment.

LMW chemotactic cytokines have been implicated in various biological processes, such as leukocyte migration, angiogenesis, hematopoiesis, atherosclerosis, and cancer migration and metastasis. CXCL7, also known as PBP, is one of the members of the angiogenic ELR^+ CXC chemokine family (33). It is reportedly produced and stored in platelets, monocytes, neutrophils, and megakaryocytes. Secreted CXCL7 binds to CXC chemokine receptor 2 (CXCR2) on endothelium and mediates angiogenesis through activation of the Ras/Raf/mitogen-activated protein kinase (MAPK) and PI3K/AKT/mTOR signaling pathways (33, 34). The histology of pancreatic ductal adenocarcinoma is often characterized by hypovascularization. The reduction of circulating CXCL7 in patients with pancreatic cancer may play a certain role in the suppression of angiogenesis.

Recently, reduction in the level of serum CXCL7 has been reported to be a biomarker for advanced myelodysplastic syndrome (35). In contrast, CXCL7 is increased in the pulmonary venous blood of lung cancer patients and is significantly decreased after curative surgical resection of the lung lesions. Of particular interest is the fact that the increment of CXCL7 is detectable several months before diagnosis of lung cancer (36). We observed a reduction of CXCL7 in 10

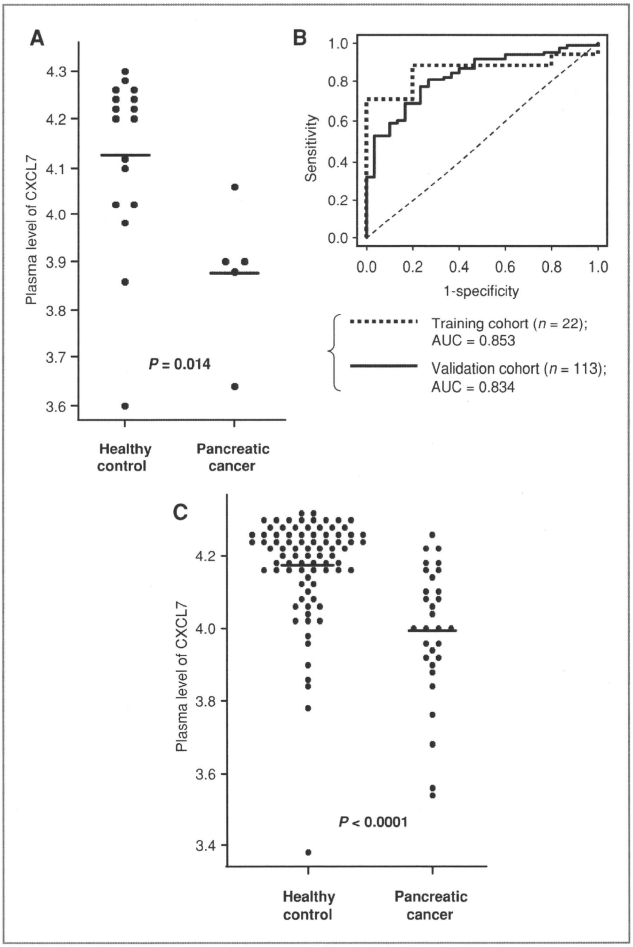

Figure 4. A and C, plasma levels of CXCL7 in healthy controls (left) and patients with pancreatic cancer (right) with the normal levels of CA19-9 (<37 U/mL) in the training (A) and validation (C) cohorts. Horizontal lines represent the average levels of CXCL7. B, ROC analyses of CXCL7 for discrimination between pancreatic cancer patients and healthy controls with normal levels of CA19-9 (<37 U/mL) in the training (dotted line) and validation (solid line) cohorts.

patients with chronic pancreatitis; but, examination of a larger number of patients will be needed before any definite conclusion can be reached.

CXCL7 is N-terminally truncated by cathepsin G-like enzymes and converted to other types of chemokines with distinct functions such as connective tissue-activating peptide III (CTAP-III) and neutrophil-activating peptide 2 (NAP-2; refs. 37, 38). One possible explanation for the reduction of plasma CXCL7 in patients with pancreatic cancer is degradation by certain exoproteases (39). Matrix metalloproteinase-9 (MMP9) has been reported to degrade CXC chemokines (40). MMP9 is often upregulated in pancreatic cancer cells and secreted into plasma (41). However, in this study, the precise molecular mechanisms behind the reduction of plasma CXCL7 in patients with pancreatic cancer remained unexplained.

Because the process of pancreatic carcinogenesis is probably mediated by various molecular pathways (42), the diagnosis of pancreatic cancer using a single biomarker may not be realistic, and a combination of different biomarkers with distinct spectra would appear to be a more realistic alternative. CA19-9 is the most widely used serum biomarker for pancreatic cancer; but, its sensitivity and specificity have been recognized to be unsatisfactory for pancreatic cancer screening (7, 12). We demonstrated that CXCL7 significantly improved the discriminatory ability of CA19-9, and this improvement was reproducibly validated in a large multi-institutional cohort. However, further independent validation by other investigators is still mandatory before its clinical application can be warranted (15, 29–31, 43).

The primary goal of the present study was to discover new biomarkers useful for the early detection of pancreatic cancer in an asymptomatic population. Aberrations of circulating CXCL7 have also been reported in other premalignant conditions. The present study has not only explored the utility of CXCL7 as a biomarker, but also provided a novel insight into the chemokine-mediated reactions that occur during early carcinogenesis.

Disclosure of Potential Conflicts of Interest

These sponsors had no role in the design of the study, the collection of the data, the analysis and interpretation of the data, the decision to submit the manuscript for publication, or the writing of the manuscript.

Acknowledgment

We thank Ms. Ayako Igarashi, Ms. Tomoko Umaki, and Ms. Yuka Nakamura for their technical assistance.

Grant Support

Program for Promotion of Fundamental Studies in Health Sciences conducted by the National Institute of Biomedical Innovation of Japan, the Third-Term Comprehensive Control Research for Cancer and Research on Biological Markers for New Drug Development conducted by the Ministry of Health and Labor of Japan.

The costs of publication of this article were defrayed in part by the payment of page charges. This article must therefore be hereby marked *advertisement in accordance with 18 U.S.C. Section 1734 solely to indicate this fact.*

Received 04/15/2010; revised 10/22/2010; accepted 11/28/2010; published OnlineFirst 12/01/2010.

References

1. Jemal A, Murray T, Samuels A, Ghafoor A, Ward E, Thun MJ. Cancer statistics, 2003. CA Cancer J Clin 2003;53:5–26.
2. Michl P, Pauls S, Gress TM. Evidence-based diagnosis and staging of pancreatic cancer. Best Pract Res Clin Gastroenterol 2006;20:227–51.
3. Ministry of Health, Labour and Welfare. Japanese Government: vital statistics of Japan2009. Available from: http://ganjoho.ncc.go.jp/professional/statistics/odjrh3000000hwsa-att/cancer_mortality(1958-2008).xls.
4. American Cancer Society. Cancer Facts and Figures2007. Atlanta, GA: American Cancer Society; 2007. p. 16–7.
5. Nitecki SS, Sarr MG, Colby TV, van Heerden JA. Long-term survival after resection for ductal adenocarcinoma of the pancreas. Is it really improving?Ann Surg 1995;221:59–66.
6. Tsuchiya R, Noda T, Harada N, et al. Collective review of small carcinomas of the pancreas. Ann Surg 1986;203:77–81.
7. DiMagno EP, Reber HA, Tempero MA. AGA technical review on the epidemiology, diagnosis, and treatment of pancreatic ductal adenocarcinoma. American Gastroenterological Association. Gastroenterology 1999;117:1464–84.
8. Nieto J, Grossbard ML, Kozuch P. Metastatic pancreatic cancer 2008: is the glass less empty?Oncologist 2008;13:562–76.
9. Burris HA 3rd, Moore MJ, Andersen J, et al. Improvements in survival and clinical benefit with gemcitabine as first-line therapy for patients with advanced pancreas cancer: a randomized trial. J Clin Oncol 1997;15:2403–13.
10. Poplin E, Feng Y, Berlin J, et al. Phase III, randomized study of gemcitabine and oxaliplatin versus gemcitabine (fixed-dose rate infusion) compared with gemcitabine (30-minute infusion) in patients with pancreatic carcinoma E6201: a trial of the Eastern Cooperative Oncology Group. J Clin Oncol 2009;27:3778–85.
11. NCCN Clinical Practice Guidelines in Oncology: Pancreatic Adenocarcinoma V.1. National Comprehensive Cancer Network; 2009.
12. Goggins M. Molecular markers of early pancreatic cancer. J Clin Oncol 2005;23:4524–31.
13. Goggins M, Canto M, Hruban R. Can we screen high-risk individuals to detect early pancreatic carcinoma?J Surg Oncol 2000;74:243–8.
14. Hanash S. Disease proteomics. Nature 2003;422:226–32.
15. Grantzdorffer I, Carl-McGrath S, Ebert MP, Rocken C. Proteomics of pancreatic cancer. Pancreas 2008;36:329–36.
16. Yamaguchi U, Nakayama R, Honda K, et al. Distinct gene expression-defined classes of gastrointestinal stromal tumor. J Clin Oncol 2008;26:4100–8.
17. Ono M, Shitashige M, Honda K, et al. Label-free quantitative proteomics using large peptide data sets generated by nanoflow liquid chromatography and mass spectrometry. Mol Cell Proteomics 2006;5:1338–47.
18. Matsubara J, Ono M, Negishi A, et al. Identification of a predictive biomarker for hematologic toxicities of gemcitabine. J Clin Oncol 2009;27:2261–8.
19. Negishi A, Ono M, Handa Y, et al. Large-scale quantitative clinical proteomics by label-free liquid chromatography and mass spectrometry. Cancer Sci 2009;100:514–9.
20. Ono M, Matsubara J, Honda K, et al. Prolyl 4-hydroxylation of alpha-fibrinogen: a novel protein modification revealed by plasma proteomics. J Biol Chem 2009;284:29041–9.
21. Anderson NL, Anderson NG. The human plasma proteome: history, character, and diagnostic prospects. Mol Cell Proteomics 2002;1:845–67.
22. Tanaka Y, Akiyama H, Kuroda T, et al. A novel approach and protocol for discovering extremely low-abundance proteins in serum. Proteomics 2006;6:4845–55.
23. Kennedy S. The role of proteomics in toxicology: identification of biomarkers of toxicity by protein expression analysis. Biomarkers 2002;7:269–90.
24. Tirumalai RS, Chan KC, Prieto DA, Issaq HJ, Conrads TP, Veenstra TD. Characterization of the low molecular weight human serum proteome. Mol Cell Proteomics 2003;2:1096–103.
25. Available from: http://www.fhcrc.org/science/international_biomarker/.
26. Honda K, Yamada T, Hayashida Y, et al. Actinin-4 increases cell motility and promotes lymph node metastasis of colorectal cancer. Gastroenterology 2005;128:51–62.
27. Idogawa M, Yamada T, Honda K, Sato S, Imai K, Hirohashi S. Poly (ADP-ribose) polymerase-1 is a component of the oncogenic T-cell factor-4/beta-catenin complex. Gastroenterology 2005;128:1919–36.

28. Matsubara J, Ono M, Honda K, et al. Survival prediction for pancreatic cancer patients receiving gemcitabine treatment. Mol Cell Proteomics 2010;9:695–704.
29. Fiedler GM, Leichtle AB, Kase J, et al. Serum peptidome profiling revealed platelet factor 4 as a potential discriminating Peptide associated with pancreatic cancer. Clin Cancer Res 2009;15:3812–9.
30. Koopmann J, Zhang Z, White N, et al. Serum diagnosis of pancreatic adenocarcinoma using surface-enhanced laser desorption and ionization mass spectrometry. Clin Cancer Res 2004;10:860–8.
31. Koopmann J, Buckhaults P, Brown DA, et al. Serum macrophage inhibitory cytokine 1 as a marker of pancreatic and other periampullary cancers. Clin Cancer Res 2004;10:2386–92.
32. Rhodes JM. Usefulness of novel tumour markers. Ann Oncol 1999;10Suppl 4:118–21.
33. Strieter RM, Burdick MD, Mestas J, Gomperts B, Keane MP, Belperio JA. Cancer CXC chemokine networks and tumour angiogenesis. Eur J Cancer 2006;42:768–78.
34. Heidemann J, Ogawa H, Dwinell MB, et al. Angiogenic effects of interleukin 8 (CXCL8) in human intestinal microvascular endothelial cells are mediated by CXCR2. J Biol Chem 2003;278:8508–15.
35. Aivado M, Spentzos D, Germing U, et al. Serum proteome profiling detects myelodysplastic syndromes and identifies CXC chemokine ligands 4 and 7 as markers for advanced disease. Proc Natl Acad Sci USA 2007;104:1307–12.
36. Yee J, Sadar MD, Sin DD, et al. Connective tissue-activating peptide III: a novel blood biomarker for early lung cancer detection. J Clin Oncol 2009;27:2787–92.
37. Ehlert JE, Ludwig A, Grimm TA, Lindner B, Flad HD, Brandt E. Down-regulation of neutrophil functions by the ELR(+) CXC chemokine platelet basic protein. Blood 2000;96:2965–72.
38. Pillai MM, Iwata M, Awaya N, Graf L, Torok-Storb B. Monocyte-derived CXCL7 peptides in the marrow microenvironment. Blood 2006;107:3520–6.
39. Villanueva J, Shaffer DR, Philip J, et al. Differential exoprotease activities confer tumor-specific serum peptidome patterns. J Clin Invest 2006;116:271–84.
40. Van Den Steen PE, Proost P, Wuyts A, Van Damme J, Opdenakker G. Neutrophil gelatinase B potentiates interleukin-8 tenfold by amino-terminal processing, whereas it degrades CTAP-III, PF-4, and GRO-alpha and leaves RANTES and MCP-2 intact. Blood 2000;96:2673–81.
41. Tian M, Cui YZ, Song GH, et al. Proteomic analysis identifies MMP-9, DJ-1 and A1BG as overexpressed proteins in pancreatic juice from pancreatic ductal adenocarcinoma patients. BMC Cancer 2008;8:241.
42. Gansauge S, Gansauge F, Beger HG. Molecular oncology in pancreatic cancer. J Mol Med 1996;74:313–20.
43. Honda K, Hayashida Y, Umaki T, et al. Possible detection of pancreatic cancer by plasma protein profiling. Cancer Res 2005;65:10613–22.

AUTHOR QUERIES

AUTHOR PLEASE ANSWER ALL QUERIES

Q1: Page 1: Per journal style, genes, alleles, loci, and oncogenes are italicized; proteins are roman. Please check thoughout to see that the words are styled correctly.

Q2: Page 1: Please check whether the affiliations are OK.

Q3: Page 10: AU/PE: Is the dislosure statement correct?

Q4: Page 10: As per the journal style, if the reference contains more than 6 authors names then it is cited as 6 authors followed by et al. Please provide 6 authors names for the following references: 6, 9, 10,16–20, 22, 26, 28–31, 34–36, 39, 41, and 43.

Q5: Page 10: Please provide the location in reference 11.

Q6: Page 10: Please provide the author names for reference 25.

AU: Below is a summary of the name segmentation for the authors according to our records. The First Name and the Surname data will be provided to PubMed when the article is indexed for searching. Please check each name carefully and verify that the First Name and Surname are correct. If a name is not segmented correctly, please write the correct First Name and Surname on this page and return it with your proofs. If no changes are made to this list, we will assume that the names are segmented correctly, and the names will be indexed as is by PubMed and other indexing services.

First Name	Surname
Junichi	Matsubara
Kazufumi	Honda
Masaya	Ono
Yoshinori	Tanaka
Michimoto	Kobayashi
Giman	Jung
Koji	Yanagisawa
Tomohiro	Sakuma
Shoji	Nakamori
Naohiro	Sata
Hideo	Nagai
Tatsuya	Ioka
Takuji	Okusaka
Tomoo	Kosuge
Akihiko	Tsuchida
Masashi	Shimahara
Yohichi	Yasunami
Tsutomu	Chiba
Setsuo	Hirohashi
Tesshi	Yamada

cathepsin D and cathepsin B proteins by western blotting (Figure S17). Moreover, the results also indicated that the molecular weights of the intramitochondrial proteins of cathepsin D and cathepsin B (M: lanes 1–10) are the same as those of the cytoplasmic proteins of cathepsin D and cathepsin B (C: lanes 11–12), implying that the intramitochondrial cathpsin D and cathepsin B are not synthesized within mitochondria, but the cytoplasmic proteins are translocated into mitochondria (Figure S17).

All these results strongly indicated that Mieap and lysosomal proteins are localized within mitochondria. Therefore, we designated this phenomenon as Mieap-induced accumulation of lysosome-like organelles within mitochondria (MALM).

Mieap-induced intramitochondrial lysosome-like organella is involved in eliminating oxidized mitochondrial proteins

Since MALM is not related to canonical autophagy of mitochondria, we speculated that MALM might be involved in degradation of the mitochondrial proteins. The expression levels of endogenous mitochondrial proteins were assessed in the Mieap$^+$ cells (Ad-Mieap–infected HCT116 and LS174T-control cells) and Mieap$^-$ cells (Ad-LacZ–infected HCT116 and LS174–Mieap-KD cells). Interestingly, F1F0-ATP synthase alpha-subunit (ATP synthase α), beta-subunit (ATP synthase β), and mitochondrial DNA-encoded NADH dehydrogenase subunit 1 (MTND1), which are located in mitochondrial matrix and innermembrane and are critical mediators for oxidative phosphorylation and energy production, slightly accumulated after IR in the Mieap$^-$ cells (Figure 8A). However, no differences in mitofilin (intermembrane space protein) and VDAC (outermembrane protein) between the Mieap$^+$ and Mieap$^-$ cells were observed (Figure 8A). These results suggest that MALM may specifically degrade some mitochondrial proteins in mitochondrial matrix and innermembrane proteins.

Since mitochondria are the main source of ROS generation in cells, the mitochondrial proteins are often oxidized and damaged by ROS [7,8,12]. Thus, we speculated that the Mieap-regulated lysosomes might specifically target and degrade the oxidized proteins in mitochondria. To confirm this hypothesis, we analyzed the oxidized protein.

First, we examined the oxidative modification of carbonyl groups in protein side chains. As shown in Figure 8B, oxidized proteins markedly accumulated in LS174T-*Mieap*-KD cells following treatment with H_2O_2 in a time-dependent manner, whereas no change in LS174T-control cells was observed. Furthermore, one of the oxidized proteins was identified as the F1F0-ATP synthas β-subunit (Figure 8C), which plays an essential role in mitochondrial ATP production. Interestingly, prior to the application of any stress, the carbonylated form of the F1F0-ATP synthase β-subunit was already increased in the Mieap$^-$ cells (Figure 8C), suggesting that MALM functions under normal basal conditions to eliminate ROS-damaged proteins in mitochondria.

Next, we examined the other oxidative modification of nitrotyrosine using anti-nitrotyrosine antibody that allows for IF analysis of the oxidized proteins. As shown in Figure 8D, both the IR and H_2O_2 treatment dramatically induced the accumulation of oxidative proteins in the mitochondria, and in part, in the cytoplasm outside of the mitochondria in the Mieap$^-$ cells (Ad-LacZ infected HCT116 and LS174T-Mieap-KD). In contrast, the Mieap$^+$ cells (Ad-Mieap-infected HCT116 and LS174T-cont) revealed much smaller changes. Consistent with the results of western blot analysis on carbonyl groups modification, even without any stresses, the Mieap$^-$ cells already revealed accumulation of nitrotyrosine-oxidized proteins in mitochondria. These results further support the role of Mieap in the maintenance of mitochondrial integrity under normal condition (Figure 8D). Collectively, the present results suggest that, in order to maintain healthy mitochondria, Mieap-induced intramitochondrial lysosome-like organella plays an important role in eliminating the oxidized mitochondrial proteins.

Mieap repairs unhealthy mitochondria

Oxidized proteins have been reported to lose their normal activity [14,33]. Therefore, it is possible that accumulation of the oxidized proteins in mitochondria may impair the function of the mitochondria, leading to the accumulation of dysfunctional and unhealthy mitochondria in the Mieap$^-$ cells. The term "unhealthy mitochondria" generally refers to mitochondria with dysfunctional oxidative phosphorylation, which is manifested by reduced ATP synthesis and the excess generation of ROS [7]. In addition, the oxidized form of the F1F0-ATP synthase β-subunit was actually accumulated in the Mieap$^-$ cells (Figure 8C). Therefore, we hypothesized that the mitochondria in the Mieap$^-$ cells might show reduced ATP synthesis and high levels of ROS.

To investigate whether the mitochondria in the Mieap-deficient cells are dysfunctional, the ATP synthesis activity of the mitochondria in the Mieap$^+$ (Ad-Mieap-infected HCT116 and LS174T-cont) and Mieap$^-$ (Ad-LacZ infected HCT116 and LS174T-Mieap-KD) cells was assessed as previously described [34]. Interestingly, the ATP synthesis activity of the mitochondria was significantly impaired in the Mieap$^-$ cells even prior to the induction of IR-mediated stress (data not shown). Moreover, the ATP synthesis activity of the mitochondria in the Mieap$^-$ cells was severely decreased following IR-treatment compared to the Mieap$^+$ cells (Figure 9A).

Further examination of the ROS generated by mitochondria in the Mieap-deficient cells, using the mitochondrial ROS indicator MitoSOX-Red (red), indicated that the mitochondrial ROS level in both Mieap$^-$ cell lines dramatically increased after IR stress in a time-dependent manner, whereas the Mieap$^+$ cells showed only a slight increase (Figure 9B). Additional experiments with another mitochondrial ROS indicator, dihydrorhodamine123 (DHR123) (green), further verified these findings (data not shown). Taken together, these results suggest that Mieap prevents the accumulation of unhealthy and dysfunctional mitochondria by eliminating the oxidized and damaged mitochondrial proteins, including ATP synthase β-subunit, thereby maintaining mitochondrial function and inhibiting the generation of mitochondrial ROS.

Discussion

Canonical autophagy of mitochondria, known as "mitophagy," is thought to play a critical role in mitochondrial quality control [10,11]. To date, studies on yeast have provided most of the information on mitophagy. Several yeast studies have suggested that mitochondrial autophagy is mediated by macroautophagy [11,35], and studies on mammalian cells have supported this finding [29,36]. In macroautophagy, double-membraned autophagosomes engulf proteins and organelles along with a portion of the cytoplasm [32]. Therefore, the process of macroautophagy is generally considered non-specific to the target proteins and organelles. However, it has been suggested that some type of mitophagy can be mediated by the selective macroautophagy of mitochondria. For example, NIX has been shown to play an essential role in the selective mitochondrial macroautophagy observed during the maturation of erythroid cells [37,38]. In cervical cancer and neuroblastoma cells, parkin and PINK1 have also been shown to play a critical role in the selective

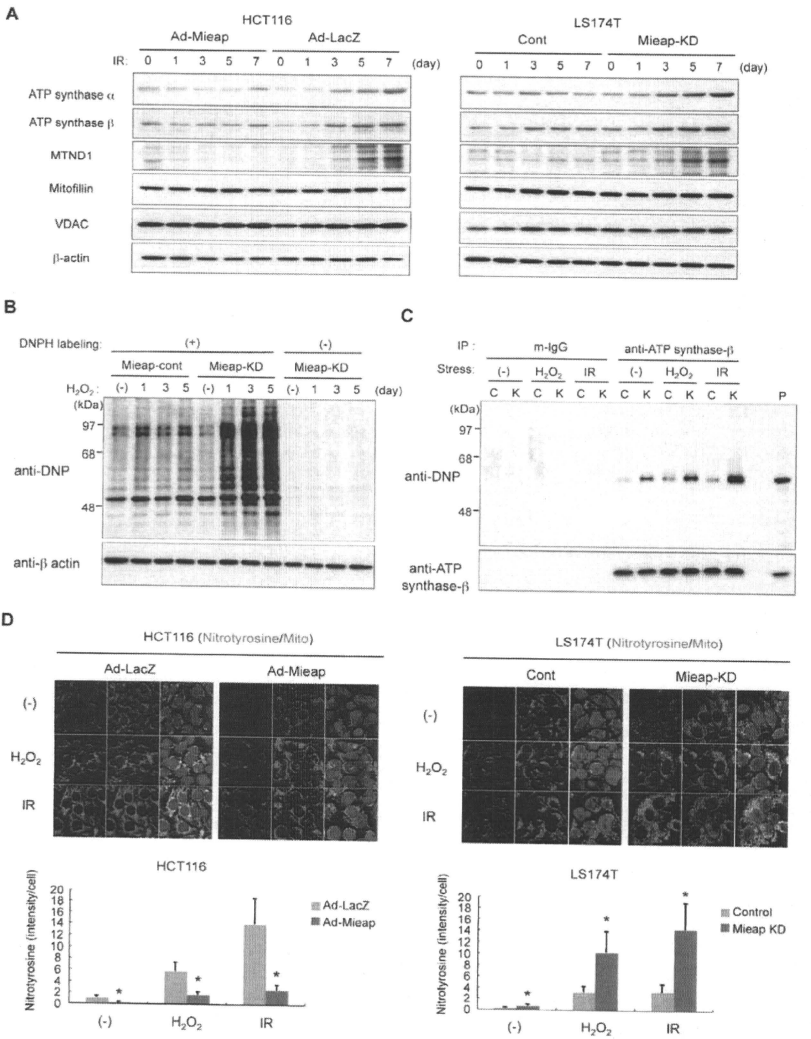

Figure 8. MALM is involved in elimination of mitochondrial oxidized proteins. (A) Expression levels of endogenous mitochondrial proteins. The Ad-Mieap- or Ad-LacZ-infected HCT116 cells, or the LS174T cont and Mieap-KD cells were irradiated by γ ray, and the cells were subjected to western blot analysis at the indicated times on the indicated proteins. (B) Western blot analysis of the oxidized proteins. The total cell lysates isolated

at the indicated times from the H_2O_2-treated cont and Mieap-KD cells of LS174T were labeled by DNPH, and then subjected to western blot analysis with anti-DNP antibody in order to detect the carbonyl-oxidized proteins. β-actin was used as a loading control (A) (B). (C) Western blot analysis of the oxidized ATP synthase beta-subunit protein. ATP synthase beta-subunit protein was specifically immunoprecipitated with mouse monoclonal anti-ATP synthase beta-subunit antibody from the cell lysates isolated from the non-treated (-), H_2O_2-treated (H_2O_2), or γ-irradiated (IR) cont (C) and Mieap-KD (K) cells of LS174T, and then the precipitated proteins in each group were subjected to DNPH labeling and the following western blot analysis with anti-DNP antibody. Total ATP synthase beta-subunit protein in the stripped membrane was detected with rabbit polyclonal anti-ATP synthase beta-subunit antibody as the loading control. The band of ATP synthase beta-subunit protein was shown as the positive control of the size (P). (D) IF analysis of the oxidized proteins. The Ad-Mieap- or Ad-LacZ-infected HCT116 cells, or the LS174T cont and Mieap-KD cells were irradiated by γ ray, treated with H_2O_2, or not treated, and 3 days after the treatment, the IF experiment was carried out with anti-nitrotyrosine antibody (Nitrotyrosine) in order to detect the nitrotyrosine-oxidized proteins. Mitochondria were indicated by the DsRed-mito protein signal (Mito). The representative images were shown (upper panel). Quantitative analysis of nitrotyrosine intensity was carried out in 300–400 cells. Average intensities of the nitrotyrosin-oxidized proteins per cell are shown with error bars indicating 1 standard deviation (SD; lower panel). $p<0.01$ (*) was considered statistically significant.

doi:10.1371/journal.pone.0016054.g008

macroautophagy of mitochondria [30,31]. In all these mechanisms, double-membraned autophagosomes are essential for the degradation of the entire structure of mitochondrion. In addition, the process is very rapid and is completed within a few hours [29,36]. However, in the present study, MALM continued for several days, and autophagosomes characterized by the double-membraned structure on electron microscopy (EM) and the dot signal of GFP-LC3 on immunofluorescence (IF) analysis were not related to MALM at all. Moreover, we observed neither the destruction of the mitochondrial structure on EM nor the loss of mitochondrial signal on IF analysis; these findings are usually detected in canonical autophagy of mitochondria. On the basis of these facts, we conclude that MALM is completely different from degradation of the entire mitochondrion, which is also termed mitophagy.

From the morphological viewpoint, a typical lysosomal structure in the cytoplasm is a membrane-surrounded vesicle, whose size varies from less than 1 μm (~10 nm) to several microns and whose content reveals a heterogeneous and variable pattern, which occasionally contains other organelles for digestion [16,39]. On EM, we were unable to detect this type of lysosomal structure within mitochondria. However, pre-embedding immunoelectron microscopy with DAB clearly showed that Mieap and lysosomal proteins, including LAMP1, LAMP2, cathepsin D, and cathepsin B, are located within mitochondria. In addition, post-embedding immunoelectron microscopy with gold particles also showed the presence of the Mieap, cathepsin D, and LAMP1 proteins within mitochondria. Furthermore, the results of proteinase K protection assay with the fractionated mitochondria indicated that the Mieap, cathepsin B, and cathepsin D proteins are present within mitochondria. On the basis of these facts, we concluded that atypical lysosomes or lysosome-like organelles are localized within mitochondria, without destroying the mitochondrial structure. Therefore, we speculate that the morphological structure of the Mieap-induced intramitochondrial lysosome-like organella is different from the typical lysosomal structure.

The regular structure of lysosomes is difficult to describe. In terms of morphology, lysosomes are less clearly defined than other subcellular organelles [16,39]. The lysosomal structure is variable and depends on the cell type and the actual conditions [16,39]. Even when lysosomes are visible on EM, their size varies from less than 1 μm (~10 nm) to several microns [16,39]. In particular, the minimum size of lysosomes is unknown. These findings indicate that the shape and appearance of lysosomes have not been clearly defined thus far. Mitochondria contain a number of membrane structures because of the presence of mitochondrial cristae and the inner membrane. Therefore, it appears to be difficult to determine the lysosomal structure within mitochondria by distinguishing the lysosomal membrane from the mitochondrial membrane. In particular, when a lysosome is involved in a specific degradation of proteins, such as chaperon-mediated autophagy (CMA) [19], it is much more difficult to determine the lysosomal structure because the lysosome does not contain any degraded contents of some organelle structures. Currently, it is likely that only the immunocytochemical or biochemical analysis carried out in this study can be used to detect the presence of intramitochondrial lysosome-like organella.

The presence of intramitochondrial lysosome-like organella raises many questions. One of the most important questions is how the organelles occur within mitochondria. We hypothesize that the presence of intramitochondrial lysosome-like organella can be explained via two possible mechanisms. First, cytoplasmic lysosomes or lysosome-like organelles are translocated into mitochondria without destroying the mitochondrial outer and inner membranes. Second, lysosomes or lysosome-like organelles are generated within mitochondria. We assume that the former mechanism is more plausible than the latter because the lysosomal compartment consists of at least more than 50 proteins, as mentioned. Because mitochondrial DNA does not encode lysosomal proteins, all the components of lysosomes must be imported into mitochondria before assembly. However, none of the lysosomal components have mitochondria-targeting signal sequences, implying that the proteins cannot be delivered into mitochondria. In addition, the organella is surrounded by a single membrane structure. It appears almost impossible to supply or generate the lysosomal membrane structure within mitochondria. Moreover, as shown in Figure S17, the molecular weights of the intramitochondrial proteins of cathepsin D and cathepsin B in MALM are the same as those of the cytoplasmic proteins of cathepsin D and cathepsin B, implying that the intramitochondrial cathpsin D and cathepsin B are not synthesized within mitochondria, but the cytoplasmic proteins are translocated into mitochondria. When cathepsin D and cathepsin B proteins are synthesized in cytoplasm, the proteins are targeted to lysosomes through ER-Golgi trafficking pathway. During the process, cathepsin D and cathepsin B are glycosylated. If the intramitochondrial cathepsin D and cathepsin B are synthesized within mitochondria, the intramitochondrial proteins are not glycosylated, whose molecular-weights are different from those of the cytoplasmic proteins. Therefore, taken together, we think that the latter mechanism is unfeasible and very inefficient. We speculate that cytoplasmic lysosome-like organelles are translocated into mitochondria.

Even if our hypothesis is true, it remains to be determined how lysosome-like organelles enter mitochondria without breaking down the mitochondrial structure. Several channels of the mitochondrial outer and inner membranes, which regulate the transport of mitochondrial proteins [40] or the release of cytochrome *c* from the mitochondrial intermembrane space during apoptosis [41], have been identified. None of these

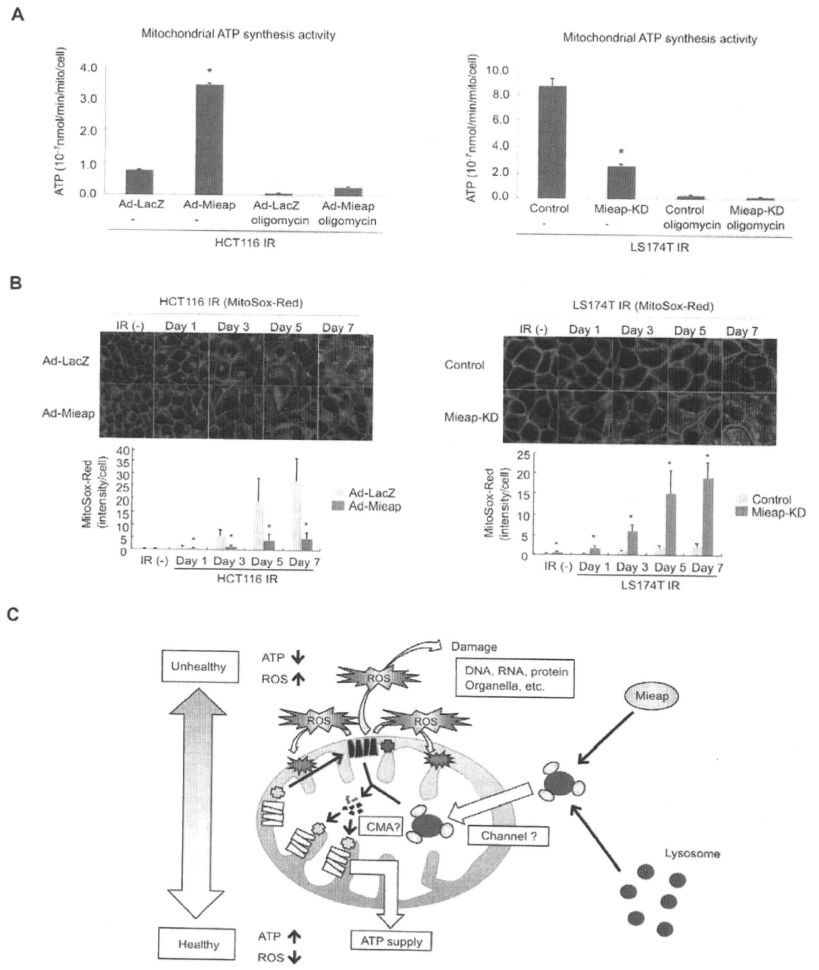

Figure 9. Mieap repairs unhealthy mitochondria. (A) ATP synthesis activity by the mitochondria. The Ad-Mieap- or Ad-LacZ-infected HCT116 cells, or the LS174T cont and Mieap-KD cells were subjected to ATP synthesis assay on day 7 after IR. Oligomycin, an inihibitor of mitochondrial oxidative phosphorylation, was used in the assay in order to detect non-mitochondrial ATP synthesis activity. The assay of each group was independently carried out three times. The average activities of ATP synthesis are shown with error bars indicating 1 SD. $p<0.01$ (*) was considered statistically significant. (B) Mitochondrial ROS level. The cells were γ ray irradiated, and the ROS generated by mitochondria in the cells was analyzed by MitoSox-Red without IR or at the indicated times after IR. The representative images are shown (upper panel). Quantitative analysis of ROS was carried out in 300–400 cells (lower panel). Average intensities of ROS per cell are shown with error bars indicating 1 SD. $p<0.01$ (*) was considered statistically significant. (C) Hypothetical model for the Mieap-regulated mitochondrial quality control.
doi:10.1371/journal.pone.0016054.g009

channels appear to explain the mechanism underlying MALM because the protein transport machinery can allow the specific transport of only individual proteins [40], and the pore of the apoptosis machinery such as VDAC seems to open a hole in only the mitochondrial outer membrane in order to release cytochrome *c* [41]. However, we speculate that a channel such as the mitochondrial permeability transition pore (MPTP) may mediate the translocation of lysosome-like organelles into mitochondria. MPTP is thought to be a nonspecific channel that spans the mitochondrial outer and inner membranes and creates a large hole between the cytoplasm and the mitochondrial matrix, leading to equilibration of H^+ across the inner membrane and mitochondrial swelling due to water influx [42]. Therefore, MPTP has been suggested to play a role in atypical cell death such as necrosis. However, the physiological role of MPTP remains unknown [42]. Because MPTP itself is permeable to solutes with a size of up to 1.5 kDa, the size of the pore seems to be too small to allow the translocation of lysosomes or lysosome-like organelles. Therefore, we speculate that an unidentified MPTP-like channel may open a large hole from the mitochondrial outer membrane to the inner membrane under the regulation of Mieap and enable translocation of lysosome-like organelles from the cytoplasm into mitochondria (Figure 9C). Further investigation is required to examine this hypothesis.

Because mitochondria produce the majority of ROS within the cell, proteins in the mitochondria are the primary targets for mitochondrial ROS and oxidative damage [8,12]. The oxidatively damaged proteins are thought to lose their normal function, which can lead to the loss of normal mitochondrial function [14,33]. Thus, the mechanism of degradation of the oxidized proteins in mitochondria appears to be important for the maintenance of mitochondrial quality. Currently, this quality control mechanism of mitochondrial proteins has not been fully characterized and only some components of the mechanism of protein degradation within mitochondria have been identified. For example, several proteases can play a critical role in this regulation of protein degradation within the mitochondria [13]. Among them, the LON protease is an important factor in the degradation of oxidized proteins in the mitochondrial matrix, including Aconitase [14,43]. In addition to LON, AAA proteases, including i-AAA and m-AAA, are also thought to be involved in the degradation of mitochondrial inner-membrane proteins [44]. Thus, these proteases play a critical role in mitochondrial protein degradation in order to maintain the quality of the mitochondria. If so, what is the role of MALM? Since the protease activities of AAA and LON primarily depend on ATP, they can function when ATP concentration is sufficient [13]. Therefore, when the cell experiences various stressful events leading to mitochondrial damage, mitochondrial ATP production may be reduced. Such conditions may result in the impairment of LON and i- or m-AAA protease function. Therefore, it is possible that the MALM system in mitochondria is a back-up system for stressful conditions, which functions to eliminate the damaged proteins within mitochondria to accelerate the repair process of unhealthy mitochondria.

In the present study, we have shown that intramitochondrial lysosome-like organella are involved in the degradation of oxidized proteins in mitochondria. The important question is how the organelles can degrade the oxidized proteins within mitochondria. We speculate that one existing mechanism may be the model mechanism underlying this function. CMA specifically degrades the oxidized proteins in cytoplasm and is one of the three major pathways in autophagy; however, it is considered an atypical function of lysosomes [19]. In this mechanism, the lysosomes can specifically uptake the oxidized proteins containing the consensus motif via the interplay of LAMP2A and heat shock protein 70 (HSP70) [19]. If the entire structure of the lysosome or lysosome-like organelles can enter and exist within the mitochondrion, MALM may function as the intramitochondrial CMA-like mechanism in order to eliminate and degrade oxidized proteins (Figure 9C).

p53 has been reported to regulate aerobic respiration by the transcriptional activation of p53 targets that are involved in the mitochondrial electron transport chain, such as SCO2 (24). In addition, p53R2, a p53 target, has been shown to regulate mitochondrial DNA synthesis [45–47]. These findings suggest that the inactivation of *p53* in human cancers leads to an impairment of aerobic respiration and mitochondrial DNA synthesis via downregulation of SCO2 and p53R2, respectively. In addition, *p53* mutations cause the accumulation of dysfunctional mitochondrial proteins via downregulation of *Mieap*. Moreover, *Mieap* expression is directly inactivated by methylation of its promoter. This causes the accumulation of unhealthy mitochondria, suggesting that these organelles in cancer cells tend to become dysfunctional. This might explain, in part, why cancer cells preferentially utilize aerobic glycolysis, as observed by Warburg [20]. Therefore, we suggest that cancer cells have a predisposition to accumulate unhealthy and dysfunctional mitochondria.

Although there are many important questions that require further study, the discovery of this unusual and important mechanism in the cell may lead to a greater understanding of the underlying mechanisms involved in various phenomena and diseases that may be a result of defective mitochondrial quality control. Moreover, our discovery raises a number of important questions regarding the well-established concepts of cell biology.

Materials and Methods

Cell lines

The following human cancer cell lines were purchased from the American Type Culture Collection: LS174T, HCT116, HT29 and Lovo (colorectal adenocarcinoma); HepG2 (hepatoblastoma); A549 and H1299 (lung cancer); MCF7 and T47D (mammary carcinoma); SKN-AS (neuroblastoma); U87MG, U138MG, U373MG and T98G (glioblastoma); HeLa (cervical cancer); SaOS2 (osteosarcoma); and Tera2 (malignant embryonal carcinoma). The TERT-immortalized normal cell line HFF2 (human fibroblast cell) was provided by T. Kiyono (National Cancer Centre Research Institute) and D.A. Galloway (Fred Hutchinson Cancer Research Centre). The LC176 cell line (lung cancer) was a gift from T. Takahashi (Aichi Cancer Centre Research Institute). Cells were cultured under the conditions recommended by their depositors.

Semi-quantitative RT-PCR analysis

The RT-PCR exponential phase was determined on 18–28 cycles, to allow semi-quantitative comparisons among complementary DNAs (cDNAs) developed from identical reactions. Each PCR regimen involved an initial denaturation step at 94°C for 5 min followed by 18 cycles (*β2-MG*), 19 cycles (*p21/WAF1*), 24 cycles (*Mieap*), 27 cycles (*ATG5* and *ATG12*) or 28 cycles (*BECN1* and *DRAM*) at 55°C for 30 s, and at 72°C for 30 s on a GeneAmp PCR system 9700 (Applied Biosystems). Primer sequences were, for *β2-MG*: forward, 5′-TAGCTGTGCTCGCGCTACT-3′ and reverse, 5′- GCGCTACTCTCTCTTCTG-3′; for *p21/WAF1*: forward, 5′- TTGGCCTGCCCAAGCTCTA-3′ and reverse, 5′-TCCTCTTGGAGAAGATCAGC-3′; for *Mieap*: forward, 5′-CTTTGCAATGCAGGCCTTAGA-3′ and reverse, 5′-CCGACTTCGAGACATCGTG-3′; for *ATG5*: forward, 5′- CTAAGGATG-